Microfluidics and Nanofluidics (2019) 23:13
https://doi.org/10.1007/s10404-018-2180-z

RESEARCH PAPER

A micro-needle induced strategy for preparation of monodisperse liquid metal droplets in glass capillary microfluidics

Qingming Hu[1,2] · Yukun Ren[1] · Xu Zheng[3] · Likai Hou[1] · Tianyi Jiang[1] · Weiyu Liu[1,4] · Ye Tao[1] · Hongyuan Jiang[1]

Received: 31 August 2018 / Accepted: 17 December 2018 / Published online: 5 January 2019

Abstract
Monodisperse micro-sized liquid metal droplets have received considerable attention for developing flexible electronics, microfluidics actuators and reconfigurable devices. Herein we report an innovative and efficient strategy for large-scale preparation of Galinstan liquid metal microdroplets with controllable sizes using a micro-needle induced glass capillary microfluidic device. By inserting a stainless steel micro-needle into the inner liquid metal phase in the glass capillary, the hydrodynamic instability of the liquid metal stream is significantly suppressed to guarantee steady fluid flow before the liquid metal is pinched off by the outer phase flow, giving rise to a stable generation of monodisperse liquid metal microdroplets. The microdroplet size dependence on the flow ratio of the continuous and dispersed-phase is investigated experimentally. A theoretical framework based on the Plateau–Rayleigh instability is proposed to explain the advantage of the micro-needle induced strategy. This strategy has great potential for the generation of high interfacial tension liquid metal emulsions.

Keywords Micro-needle induced · Liquid metal · Glass capillary microfluidic · Hydrodynamic instability · Plateau–Rayleigh instability

1 Introduction

Combined with fascinating metallic characteristics and fluidic properties, such as large surface tension, high electrical and thermal conductivities, low viscosity, and significant deformability, room temperature liquid metals have received considerable research interest recently. In contrast to mercury, low melting point gallium based eutectic liquid metals such as EGaIn (75% gallium, 25% indium) and Galinstan (68.5% gallium, 21.5% indium, and 10% tin) are being increasingly investigated by research community in laboratories for its negligible vapour pressure and nontoxicity (Chiechi et al. 2008; Hu et al. 2017; Shay et al. 2018). These remarkable physicochemical properties enable gallium-based liquid metals great promise for a variety of practical application including fluidic actuators (Tang et al. 2015, 2014a, b), electrochemical sensors (Wei et al. 2014), optical and electrical switches (Sen and Chang-Jin 2009; Wissman et al. 2017; Yoo et al. 2011), reconfigurable/stretchable electronics (Cheng et al. 2009; Dickey 2017; Liang et al. 2017), and biomedicine (Lu et al. 2015). Particularly, the growing

This article is part of the topical collection "2018 International Conference of Microfluidics, Nanofluidics and Lab-on-a-Chip, Beijing, China" guest edited by Guoqing Hu, Ting Si and Zhaomiao Liu.

Electronic supplementary material The online version of this article (https://doi.org/10.1007/s10404-018-2180-z) contains supplementary material, which is available to authorized users.

✉ Yukun Ren
rykhit@hit.edu.cn

✉ Xu Zheng
zhengxu@inm.imech.ac.cn

✉ Hongyuan Jiang
jhy_hit@hit.edu.cn

[1] School of Mechatronics Engineering, Harbin Institute of Technology, West Da-zhi Street 92, Harbin 150001, Heilongjiang, People's Republic of China

[2] School of Mechatronics Engineering, Qiqihar University, Wenhua Street 42, Qiqihar 161006, Heilongjiang, People's Republic of China

[3] State Key Laboratory of Nonlinear Mechanics, Institute of Mechanics, Chinese Academy of Sciences, No.15 Beisihuanxi Road, Beijing 100190, People's Republic of China

[4] School of Electronics and Control Engineering, Chang'an University, Middle-Section of Nan'er Huan Road, Xi'an 710064, Shaanxi, People's Republic of China

trends in the miniaturization of microfluidic reaction engineering and the development of lab-on-a-chip analysis for their flexible integration into microfluidics have facilitated the expansion of micro and nano-sized liquid metal droplets demand from the traditional polydispersed emulsions to precision monodispersity.

To date, there are several approaches have been exploited for producing micro-sized liquid metal droplets, including molding (Mohammed et al. 2014), acoustic wave (Tang et al. 2016), sonication (Hohman et al. 2011; Lu et al. 2015), stream jetting (Yu et al. 2014), electro-hydrodynamic shooting (Fang et al. 2014), and microfluidic flow focusing (Gol et al. 2016; Thelen et al. 2012). With good rheological properties, the replica molding technique featured by spreading liquid metal across the elastomeric patterned cylindrical reservoirs was demonstrated to create microspheres (Mohammed et al. 2014). Although the replication method is simple, the demand of mass production limits its pervasive application. Another commonly encountered and efficient option for large-scale microdroplet production is sonication dispersion method (Lu et al. 2015), which exploits ultrasonic wave to fabricate liquid metal marble spheres in a nonsolvent for different durations. Despite the advantages of the sonication technique for microdroplet formation, this approach suffers from a drawback that the liquid metal droplet diameter is commonly with a wide size distribution, ranging from dozens of nanometers to several micrometers. Additionally, the acoustic wave-induced-forces were introduced to generate EGaIn microdroplets with controllable size by tuning the interfacial tension of the liquid metal with either electrochemistry or electrocapillary accompanied with an electrical potential. Whereas the acoustic wave generation equipment is relatively high-cost consumption and the droplet production platform is complex. To solve the aforementioned limitations, the special microfluidic flow-focusing method has been extensively investigated to improve the reproducibility and the uniformity of the liquid metal microspheres. It is typically demonstrated by designing a PDMS microfluidic system with a cross-like microchannel configuration and producing microdroplets by adjusting the shear rate or interfacial tension of the two adjacent insoluble streams. The main problem with this approach is the hydrodynamic instability for the droplet formation, caused by the high pressure drop and the corresponding high shear rate within the microchannel. On the other hand, the swelling of PDMS-based microchannel in most organic solvents may sometimes disrupt the micrometer-sized features and make it not so easy to maintain a good uniformity of the liquid metal microdroplets. Whereas the formation of the highly monodisperse bulk liquid metal emulsions is the central technical issue in some occasions. To achieve this goal, a potential strategy is to exploit the glass capillary microfluidic approach (Hou et al. 2017; Jia et al. 2018; Lee and Weitz 2008; Shah et al. 2008; Shum et al. 2008), which has competitive advantage on precise control over the size distribution of microdroplet. However, owing to its extraordinary large surface tension, stable generation of monodispersed liquid metal microdroplet emulsion is challenging with the conventional co-flow capillary microfluidic device. Consequently, it is still of great importance to explore novel and simple methods for large-scale preparation of liquid metal microdroplets with high interfacial tension.

In this technical innovation, we introduce a novel strategy to achieve highly monodispersed microspherical Galinstan liquid metal with controllable size, by simply inserting a metallic micro-needle into the inner fluid phase of the co-flowing glass capillary device (Fig. 1d, e). In the commonly used co-flowing device (as shown in Fig. 1a, b), due to the high surface tension of the liquid metal and its weak wettability on the glass wall (Davis and Ndao 2018), the inner stream will easily break up even before flowing out of the small aperture. A specific advantage of the new design (Fig. 1d, e) is that the micro-needle can induce significant viscous effect to overcome the hydrodynamic instability of the liquid metal stream when the inner phase is pinched off by the continuous phase. To control the droplet size, a series of experiments are conducted with different flow rate ratios of continuous phase to the dispersed phase, i.e., $\varphi = Q_c/Q_d$. This strategy provides a significant guide for the large-scale production of size-controllable monodisperse liquid metal with high surface tension in laminar flow.

2 Experimental setup

2.1 Materials

Metallic micro-needle with a diameter of 70 μm is adopted (Zongsheng, Harbin, China). Glycerol is purchased from Aladdin. Poly(vinyl alcohol) (PVA, 87–89% hydrolyzed, average $M_w = 13{,}000 - 23{,}000$) and galinstan liquid metal are obtained from Sigma-Aldrich. As the out phase, a mixture of glycerol and 5% PVA aqueous solution with the weight ratio 10:2.9 is used. The inner phase is the bulk galinstan liquid metal.

2.2 Fabrication of glass capillary microfluidic device within inserted micro-needle

As illustrated in Fig. 1a, d, the glass microcapillary chip consisting of coaxial assemblies of round and square glass capillaries on glass slides is utilized to prepare the liquid metal droplets. The two cylindrical capillaries (inner diameter (ID) 0.58 mm, outer diameter (OD) 1.03 mm, World precision instruments, Inc., 1B100-6) are tapered to the desired sizes using a micropipette puller (P-97, Sutter

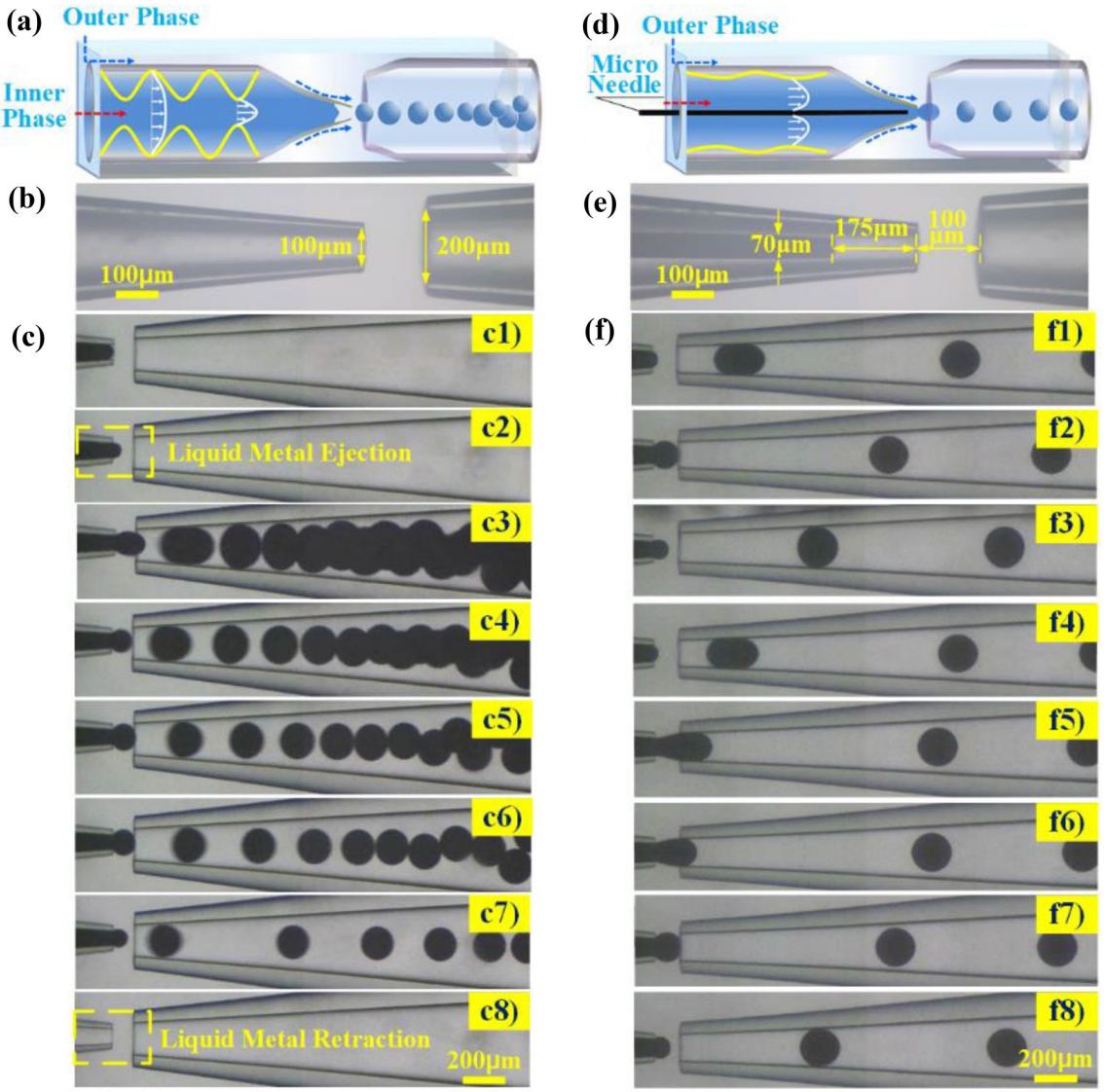

Fig. 1 Schematic illustration of the working mechanism for Galinstan liquid metal microdroplets generation. **a** The traditional co-flow microcapillary device, **b** micrograph of the tapered end of the injection and collection tube. **c** High-speed sequential snapshots of polydispersed liquid metal emulsions formation in traditional co-flow microcapillary device. **d** The proposed micro needle induced microcapillary device, **e** micrograph of the proposed micro-needle induced microcapillary. **f** High-speed sequential snapshots of stabilized generation of monodisperse liquid metal microdroplets in micro-needle induced co-flow microcapillary device

Instrument) and a microforge (MF-900, Narishige, Tritech Research, Inc). The inner diameters of tapered orifices of the capillaries for the inner phase and for final emulsions collection are 100 μm and 200 μm, respectively. Then these tapered capillaries, one with smaller orifice diameter being injection tube and the other being collection tube, are coaxially assembled in the opposite ends of the square capillary (AIT Glass, Inc., 810-9917) with axial spacing of 100 μm. To demonstrate our novel strategy, a micro-needle is assembled into the microfluidic device to stabilize the generation process of liquid metal droplets. We utilize a properly treated 1Cr18Ni19Ti stainless steel micro-needle with a diameter of 70 μm as the micro needle, which is coxially inserted into the inner phase capillary and maintain a distance of about 175 μm between the adjacent ends of the micro-needle and injection tube (as shown in Fig. 1e). As the oil film exiting on the needle surface may intervene the interface contact between the micro-needle and the inner phase liquid metal, we first rinsed the micro-needle with acetone and then dropped it in an alcohol solution to remove oil layer by ultrasonic method to ensure direct contact. Finally, a transparent epoxy resin (Devcon 5 min Epoxy) is used to seal all tubes and micro-needle when necessary. No surface modification of the capillaries

and the micro-needle is necessary during the flow focusing, which reduces the experimental variability.

2.3 Micro-needle induced microfluidic fabrication of liquid metal droplets

To generate the liquid metal droplets, we utilize the bulk galinstan liquid metal and an aqueous solution containing a 10:2.9 by weight ratio mixture of glycerol and PVA solution as disperse phase and continuous phase, respectively. The PVA is chosen as a surfactant to be added into the glycerol aqueous solution to prevent droplets against spontaneous coalescence. Two glass syringes (Hamilton) containing two different phases are installed onto syringe pumps (Harvard Apparatus) and connected to the corresponding inlets of the device. And then the inner and out phases are injected into the glass device at a constant flow rate through the injection tube and the interstice between the injection tube and square capillary, respectively. Instead of forming a spherical droplet on the glass substrate with a large contact angle, Galinstan amalgamates metals on the metal surface (Tang et al. 2014b). When pairs of immiscible fluids simultaneously flow across the capillary tip, by carefully adjusting the flowrates of each phase, droplets can be created as the less viscous liquid metal is pinched off by the highly viscous glycerol aqueous solutions. A series of experiments show that the flow rates for relatively steady droplets production to be 5–15 μl/min for Galinstan and 100–1800 μl/min for the glycerol solution.

3 Results and discussion

3.1 Restriction of the Plateau–Rayleigh instability by micro-needle-induced viscous effect

The liquid metal manifests very weak wettability on the glass surface, while the outer phase aqueous solution is easiy to wet the glass surface. Therefore, in the inner capillary, the liquid metal interface will destabilize spontaneously under a small perturbation. When there is no micro-needle involved, the development of the perturbation can be approximately described by the Plateau–Rayleigh (P–R) instability. This theory results in a characteristic time of the instability $\tau_0=(\rho R^3/\gamma)^{1/2}$, determined by the equilibrium between the streamwise flow $\rho R/{\tau_0}^2$ and the capillary effect γ/R^2. Here, R, ρ, and γ are the radius, density, and surface tension of the liquid metal jet stream.

However, the flow dynamics is obviously different when a micro-needle is introduced. The viscous effect is increased dramatically due to the friction of the needle surface and the corresponding enhancement of the shear rate in the inner phase flow. The situation when the micro-needle with radius r is introduced is illustrated in Fig. 2.

Now assuming the perturbation profile of the liquid metal jet is $e=e_0+\Delta e\cos(x/\lambda)$, the Laplace equation expresses the capillary pressure across the interface:

$$\Delta p = C\gamma = \gamma\left(\frac{1}{e+r}-\frac{\frac{\mathrm{d}^2e}{\mathrm{d}x^2}}{\left(1+\left(\frac{\mathrm{d}e}{\mathrm{d}x}\right)^2\right)^{\frac{3}{2}}}\right)\approx\gamma\left(\frac{1}{e+r}-\frac{\mathrm{d}^2e}{\mathrm{d}x^2}\right). \tag{1}$$

According to the Poiseuille equation the $Q=\frac{G}{12\mu}\frac{\Delta p}{\Delta x}$, where $\mu=0.002$ Pa s is the viscosity of the liquid metal (Sivan et al. 2013), and G is the geometry parameter describing the flow, we obtain the flow rate equation:

$$Q=\frac{G\gamma}{12\mu}\frac{\Delta e}{\lambda}\sin\frac{x}{\lambda}\left(\frac{1}{R^2}-\frac{1}{\lambda^2}\right), \tag{2}$$

where $R\approx e+r$. The conservation of the mass requires $\frac{\partial Q}{\partial x}=-\frac{\partial e}{\partial t}$, which leads to the following equation by substituting (2) and $e=e_0+\Delta e\cos(x/\lambda)$:

$$\frac{\partial\Delta e}{\partial t}=\frac{G\gamma}{12\mu}\frac{\Delta e}{\lambda^2}\left(\frac{1}{R^2}-\frac{1}{\lambda^2}\right). \tag{3}$$

Equation (3) indicates the existence of a critical perturbation wavelength $\lambda_c=R$, below which the perturbation will grow as $\partial\Delta e/\partial t>0$. We emphasize that this result is consistent with the traditional P–R instability analysis.

Furthermore, Eq. (3) implicitly introduces the characteristic time of the instability τ_{needle}. Considering the influence of the contraction section of the inner phase capillary, we obtain the expression of τ_{needle}:

$$\tau_{\mathrm{needle}}=\frac{48R^2L^2\mu}{\gamma\delta^3}, \tag{4}$$

where δ is the average thickness of the liquid metal stream, $\delta=(R(x_1)+R(x_2)-2r)/2$, $R(x_1)$ and $R(x_2)$ are the inner

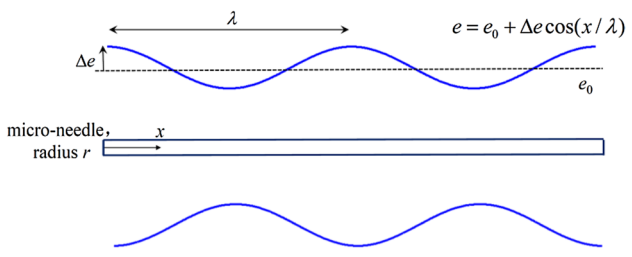

Fig. 2 A schematic diagram of the instability of the liquid metal stream in the inner phase flow

radiuses of the tapered end on the different sides. L is tapered-end's length of the injection tube.

The stability of liquid metal droplet generation is closely related to the characteristic time of the P–R instability. Specifically, a longer characteristic time indicates a more stable generation performance. To demonstrate the significantly enhanced stability of droplet formation in the proposed design, the time ratio $\xi_\tau = \tau_{\text{needle}}/\tau_0$ is defined as follow:

$$\xi_\tau = \frac{\tau_{\text{needle}}}{\tau_0} = \frac{\frac{48R^2L^2\mu}{\gamma\delta^3}}{(\rho R^3/\gamma)^{1/2}} = \frac{48R^{0.5}L^2\mu}{\delta^3\sqrt{\rho\gamma}}. \quad (5)$$

Substituting the parameters based on the experimental values: $\gamma = 0.534$ N/m (Gol et al. 2015), $R = 290$ μm, $L \approx 3$ mm, $\delta \approx 100$ μm, we can calculate that ξ_τ is about 251.84. Therefore, the needle-induced viscous effect can increase the characteristic time of instability up to two orders of magnitude. Our novel microfluidic flow focusing device with the micro-needle can work much more stable and the droplet generation is only determined by the pinch-off process excluding the influence of the instability.

3.2 The effect of micro-needle on liquid metal droplet generation

To verify the function of the micro-needle in the liquid metal droplet formation, we carry out the large-scale microdroplets generation in the hydrodynamic focusing microfluidic device without and with a metal needle. The flowrates for the dispersed and continuous phase are maintained at 10 μl/min and 300 μl/min, respectively, i.e., $\varphi = 30$. As the capillary effect is dominant in this microsystem, the contact angle and interfacial tension play key roles in droplet formation. As illustrated in Fig. 1a, when there is no micro-needle in the inner phase capillary, the droplets generation process appears to be unstable, rendering a cluster of highly ununiform droplets jetting from the nozzle in 0.5 ms, and then the liquid metal retracted back toward the inner capillary (Fig. 1c, Movie S1, ESI†). After a few seconds interval during the liquid metal re-fills the inner capillary, the droplet formation repeats the aforementioned process. One of the possible reasons is attributed to the weak surface wettability between the liquid metal and the glass wall. It can also be ascribed to the fluidic self-perturbance occurs when the liquid metal is cutting off due to the combination of the high interfacial tension and the existence of oxidation film on the liquid metal surface, which causes further unevenness in the diameters of the droplets (Fig. 3a). While with the micro-needle inside the inner phase capillary, the Galinstan microdroplets can be generated steadily and periodically with the identical droplet gap (Fig. 1f, Movie S2, ESI†). As the Galinstan liquid metal is injected along the embedded micro-needle, a large number of droplets with uniform size-distribution can be quickly fabricated (Fig. 3c). The unstable process occurring in the experiment without using the needle is never observed here. The liquid metal wets the micro-needle easily because of their similar hydrophilic properties, and thus maintain the minimal total interfacial energies of the inner phase. In particular, as we explain later, the significant improvement of the new setup is attributed to the viscous effect induced by the needle. To quantify the dimensional homogeneity of the droplet, the histograms displaying the diameter distribution for the above two approaches are shown in Fig. 3b, d. It can be found that the average droplet diameter for the conventional capillary device and the new proposed strategy are approximately 181 μm and 168 μm, respectively. While the variance of the droplet diameter normal distribution for the novel approach is 2.19, which is much smaller than the conventional droplet production method 18.03, testifying that the micro-needle induced generation approach has greater potential to produce homogeneous high interfacial tension droplet.

To demonstrate the effect of surface wettability for micro-needle on the droplet generation process, we then construct the micro-needle induced co-flowing microfluidic device with round glass rod having the identical diameter as metallic micro-needle in the inner phase capillary. As expected, with a round glass rod induced method, the liquid metal cannot flow out smoothly with lower flowrate ratio of the continuous phase to the disperse phase as $\varphi = 30$, exhibiting congestion phenomenon and a cluster of liquid metal suddenly appearing in the vicinity of the capillary tip. The small droplets are formed at a higher rate with nonperiodic breakup, when the internal flow and external phase flow velocity are maintained at 10 μl/min and 300 μl/min, respectively. Simultaneously, the continuously phase eventually flowed into the inlet capillary, forcing the liquid metal to regress back into the inlet channel and giving rise to the generation of satellite droplets (Fig. 3e). Compared with the normal distribution of the droplet diameter for the above two approaches (Fig. 3d, f), it can be clearly seen that the droplets produced with the metal needle have much better uniformity. Since Galinstan liquid metal has more similar material properties with the metallic micro-needle than the glass, which may give better wettability performance for droplet movement and adsorption on a microfiber media (Fang et al. 2015; Jamali et al. 2018; Manzo et al. 2016). Therefore, it can be probably attributed to the better wettability between the liquid metal and the metallic micro-needle than with the glass capillary, which greatly affects the stability of droplet formation.

The unstable breakup without the presence of the micro-needle reported above can be explained under the theoretical framework of the Plateau–Rayleigh instability (the Reynolds number $Re = \rho v d/\mu \sim O(1)$, ρ is the density

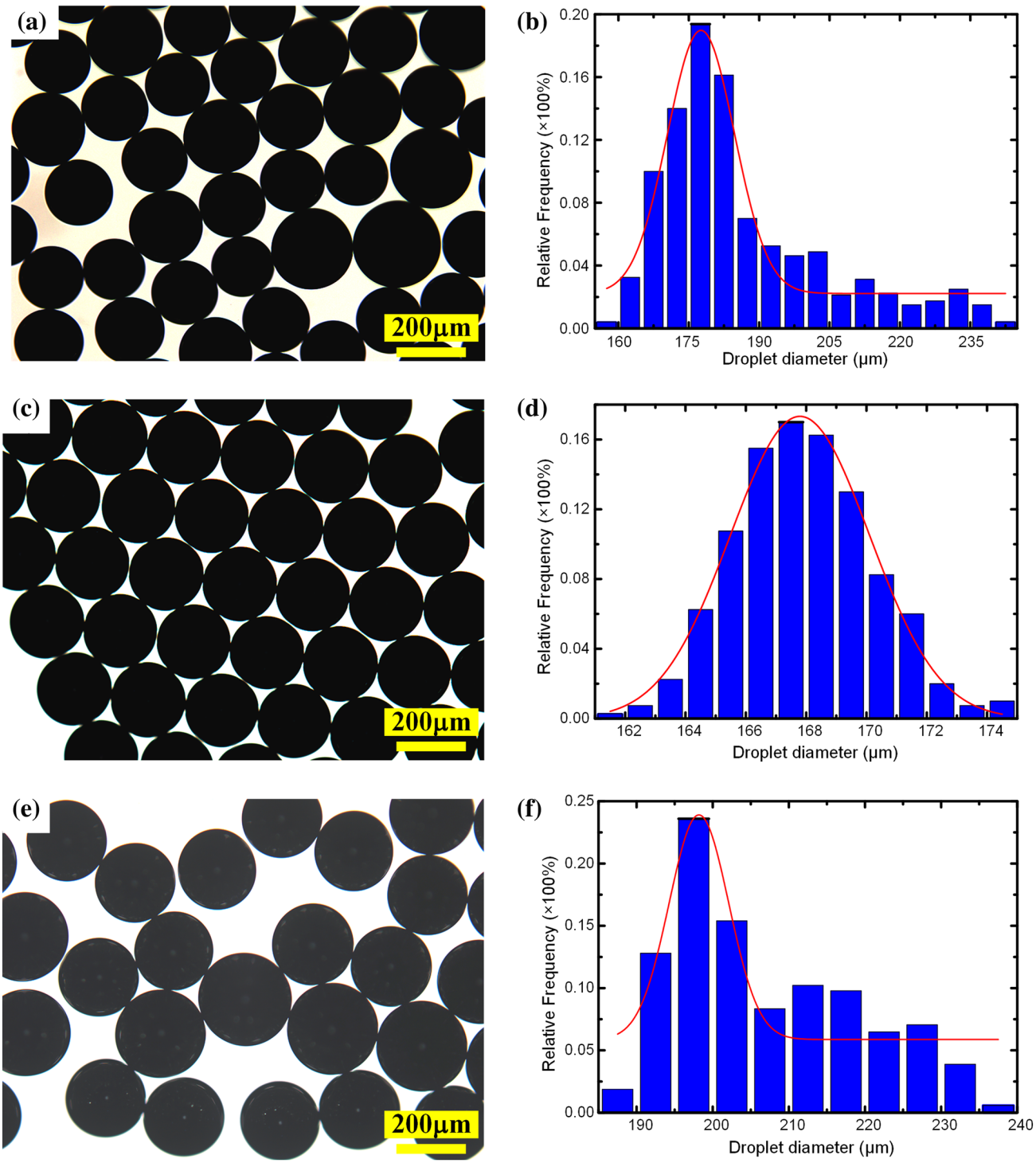

Fig. 3 Fabricated micro-sized liquid metal droplet using conventional co-flow capillary microfluidics method and the novel capillary microfluidics with micro-needle in the inlet, when the flow rates of disperse phase and continuous phase are maintained at 10 µl/min and 300 µl/min, respectively. **a** Microscopy image showing a sample of polydisperse liquid metal droplets and **b** diameter distribution histogram produced with conditional co-flow capillary microfluidics method. **c** Microscopic image showing a sample of monodisperse liquid metal microspheres and **d** diameter distribution histogram generated with novel capillary microfluidics with metallic micro-needle induced. **e** Microscopic image showing a sample of polydisperse liquid metal microspheres and **f** diameter distribution histogram generated using a round glass rod instead of a metallic micro-needle

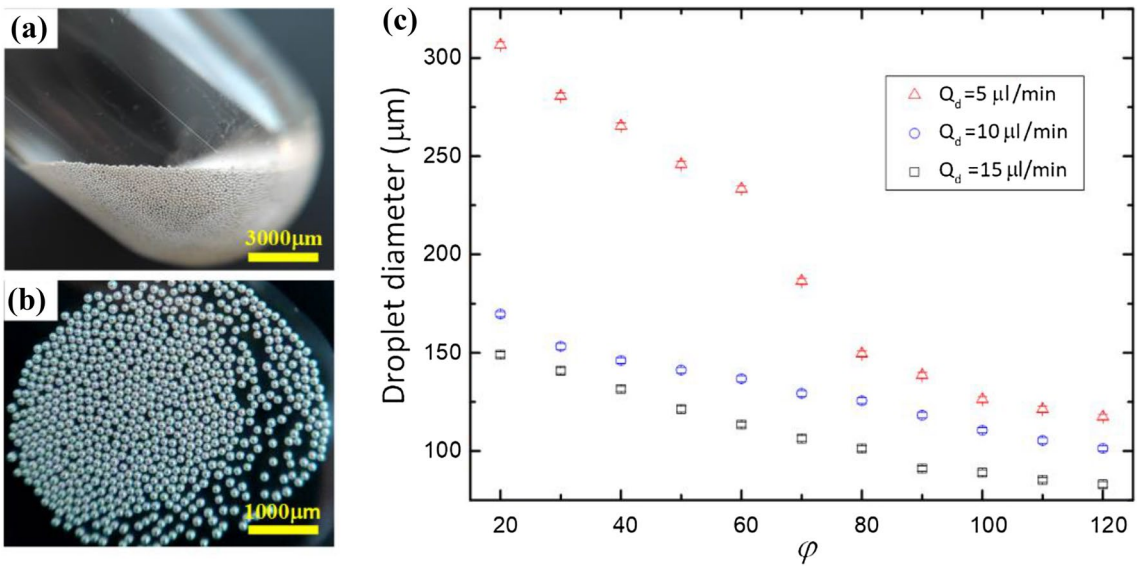

Fig. 4 Fabricated liquid metal microspheres using micro-needle induced approach. **a, b** Are optical images of liquid metal collected from the micro-needle induced capillary device. **c** Plot of liquid metal droplet size versus the flowrate ratios of continuous phase to the disperse phase

of liquid metal, v is the average flow rate, d is the equivalent diameter). This becomes a serious problem because of the very high surface tension ($\sigma = 0.534$ N/m, one order of magnitude larger than water, and the capillary number $Ca = \rho v/\gamma \sim O(10^{-6})$, γ is the surface tension) of the liquid metal and the very weak wettability of the liquid metal on the glass wall. Considering the inner phase liquid metal as a cylindrical liquid jet, the characteristic time of the instability is approximately $\tau_0 = (\rho R^3/\gamma)^{1/2}$ (de Gennes et al. 2004), which is only about 0.3 ms. This value explains the reason of the rapid breakup of the liquid metal within about 0.5 ms that generates a cluster of nonuniform droplets after being pinched off by the outer phase flow. However, the flow dynamics is obviously different when a micro-needle is introduced. The viscous effect is increased dramatically due to the friction of the needle surface and the corresponding enhancement of the shear rate in the inner phase flow. We have performed a theoretical deduction to show that the needle-induced viscous effect can increase the characteristic time of instability τ_{needle} up to two orders of magnitude, i.e., approximately 0.1 s. Therefore, the microfluidic flow focusing device with a micro-needle can work much more stable and the droplet generation is only determined by the pinch-off process excluding the influence of the instability. Nonetheless, the weak wettability of the glass rod surface introduces additional fluctuation of the interface of the metal liquid stream near the rod, which will disrupt the stream and cause the generation of polydisperse microdroplets.

3.3 The effect of flowrates ratios on liquid metal droplet diameter

To demonstrate the flexibility of our newly proposed metallic micro-needle induced approach, we controllably fabricate the Galinstan liquid metal emulsions with different sizes by tailoring the flowrates of the continuous to dispersed-phase flow rates ratios φ. Large-scale preparation of liquid metal microspheres can be accomplished with this approach (as shown in Fig. 4a, b). As illustrated in Fig. 4c, with increasing flowrate ratio φ, the droplet diameter decreases from 306.6 μm at $\varphi = 20$ to 117.4 μm at $\varphi = 120$ where the disperse phase velocity is maintained at 5 μl/min. The droplet diameter's variance tendency is resemblant with the increasing flowrate ratio for different inner phase flow velocity, namely that the average droplet diameter decreases relative dramatically when the flow-ratio φ is below 70 and then diminishes slowly with the increasing φ. The liquid metal droplet diameter varies with the flowrate ratio φ is in good agreement with previous research which studied the droplet formation regularity using a microcapillary device (Utada et al. 2005). Furthermore, smaller droplet with a diameter of 83 μm is obtained by increasing the inlet flow velocity to be 15 μl/min. The results show that the micro-needle induce technique offers an advanced platform for achieving uniformly distributed liquid metal droplets, which may help design and fabricate high performance miniaturized microfluidic actuators, electrical switches and so on.

4 Conclusion

In summary, we have demonstrated a convenient and reliable micro-needle induced glass capillary microfluidic device with a metallic micro-needle embedded into the inner phase capillary for large-scale preparation of Galinstan liquid metal microdroplets with good monodispersity. This distinct method is effective to overcome the Plateau–Rayleigh instability of the capillary-dominant microscale flow. When liquid metal with high interfacial tension flows along the micro-needle with suitable surface wettability, the micro-needle will introduce crucial viscous effect to restrict the hydrodynamic instability of the inner phase stream, eventually leading to the stable generation of monodispersed liquid metal droplets. By comparing the metal micro-needle and glass rod induced approach, we find that the good surface wettability between materials are also dominant in the breakup of the liquid metal. Through tuning the flow rate ratio of continuous and disperse phase, we can achieve the liquid metal microspheres of different sizes. Our strategy exhibits highly controllable flexibility and allows precise control of droplet size, which has a great potential in high-throughput fabrication of uniformly droplet emulsion with high surface tension.

Acknowledgements This work was supported by the National Natural Science Foundation of China (Grant nos. 11672095, 11802078, 11702035 and 11572335), the Foundation for Innovative Research Groups of the National Natural Science Foundation of China (Grant no. 51521003), the CAS Key Research Program of Frontier Sciences (QYZDB-SSW-JSC036), the CAS Strategic Priority Research Program (XDB22040403), and University Nursing Program for Young Scholars with Creative Talents in Heilongjiang Province (Grant no. UNPYSCT-2018104).

References

Cheng S, Rydberg A, Hjort K, Wu Z (2009) Liquid metal stretchable unbalanced loop antenna. Appl Phys Lett 94:144103. https://doi.org/10.1063/1.3114381

Chiechi RC, Weiss EA, Dickey MD, Whitesides GM (2008) Eutectic gallium–indium (EGaIn): a moldable liquid metal for electrical characterization of self-assembled monolayers. Angew Chem Int Ed Engl 47:142–144. https://doi.org/10.1002/anie.200703642

Davis E, Ndao S (2018) On the wetting states of low melting point metal Galinstan® on silicon microstructured surfaces. Adv Eng Mater 20:1700829

de Gennes P-G, Brochard-Wyart F, Quere D (2004) Capillarity and wetting phenomena: drops, bubbles, pearls, waves. Springer, New York, pp 119–122

Dickey MD (2017) Stretchable and Soft Electronics using. Liq Met Adv Mater 29:1606425 doi. https://doi.org/10.1002/adma.201606425

Fang W-Q, He Z-Z, Liu J (2014) Electro-hydrodynamic shooting phenomenon of liquid metal stream. Appl Phys Lett 105:134104. https://doi.org/10.1063/1.4897309

Fang J, Davoudi M, Chase G (2015) Drop movement along a fiber axis due to pressure driven air flow in a thin slit. Sep Purif Technol 140:77–83

Gol B, Tovar-Lopez FJ, Kurdzinski ME, Tang SY, Petersen P, Mitchell A, Khoshmanesh K (2015) Continuous transfer of liquid metal droplets across a fluid–fluid interface within an integrated microfluidic chip. Lab Chip 15:2476–2485. https://doi.org/10.1039/c5lc00415b

Gol B, Kurdzinski ME, Tovar-Lopez FJ, Petersen P, Mitchell A, Khoshmanesh K (2016) Hydrodynamic directional control of liquid metal droplets within a microfluidic flow focusing system. Appl Phys Lett 108:164101. https://doi.org/10.1063/1.4947272

Hohman JN, Kim M, Wadsworth GA, Bednar HR, Jiang J, LeThai MA, Weiss PS (2011) Directing substrate morphology via self-assembly: ligand-mediated scission of gallium–indium microspheres to the nanoscale. Nano Lett 11:5104–5110. https://doi.org/10.1021/nl202728j

Hou L, Ren Y, Jia Y, Deng X, Liu W, Feng X, Jiang H (2017) Continuously electrotriggered core coalescence of double-emulsion drops for microreactions ACS. Appl Mater Interfaces 9:12282–12289. https://doi.org/10.1021/acsami.7b00670

Hu L, Li J, Tang J, Liu J (2017) Surface effects of liquid metal amoeba. Sci Bull 62:700–706. https://doi.org/10.1016/j.scib.2017.04.015

Jamali M, Tafreshi HV, Pourdeyhimi B (2018) Droplet mobility on hydrophobic fibrous coatings comprising. Orthogonal Fibers Langmuir 34:12488–12499

Jia Y et al (2018) Electrically controlled rapid release of actives encapsulated in double-emulsion droplets. Lab Chip 18:1121–1129. https://doi.org/10.1039/c7lc01387f

Lee D, Weitz DA (2008) Double emulsion-templated nanoparticle colloidosomes with selective. Permeab Adv Mater 20:3498–3503. https://doi.org/10.1002/adma.200800918

Liang S et al (2017) Liquid metal sponges for mechanically durable, all-soft, electrical conductors. J Mater Chem C 5:1586–1590. https://doi.org/10.1039/c6tc05358k

Lu Y et al (2015) Transformable liquid-metal nanomedicine. Nat Commun 6:10066. https://doi.org/10.1038/ncomms10066

Manzo GM, Wu Y, Chase GG, Goux A (2016) Comparison of nonwoven glass and stainless steel microfiber media in aerosol coalescence filtration. Sep Purif Technol 162:14–19

Mohammed M, Xenakis A, Dickey M (2014) Production of liquid metal. Spheres Molding Met 4:465–476. https://doi.org/10.3390/met4040465

Sen P, Chang-Jin K (2009) A fast liquid-metal droplet microswitch using EWOD-driven contact-line sliding. J Microelectromech Syst 18:174–185. https://doi.org/10.1109/jmems.2008.2008624

Shah RK et al (2008) Designer emulsions using microfluidics. Mater Today 11:18–27. https://doi.org/10.1016/S1369-7021(08)70053-1

Shay T, Velev OD, Dickey MD (2018) Soft electrodes combining hydrogel and liquid metal. Soft Matter 14:3296–3303. https://doi.org/10.1039/c8sm00337h

Shum HC, Lee D, Yoon I, Kodger T, Weitz DA (2008) Double emulsion templated monodisperse phospholipid vesicles. Langmuir 24:7651–7653. https://doi.org/10.1021/la801833a

Sivan V, Tang S-Y, O'Mullane AP, Petersen P, Eshtiaghi N, Kalantarzadeh K, Mitchell A (2013) Liquid metal marbles. Adv Funct Mater 23:144–152. https://doi.org/10.1002/adfm.201200837

Tang S-Y et al (2014a) Liquid metal enabled pump. Proc Natl Acad Sci 111:3304–3309

Tang SY et al (2014b) Liquid metal actuator for inducing chaotic advection. Adv Funct Mater 24:5851–5858

Tang J, Zhou Y, Liu J, Wang J, Zhu W (2015) Liquid metal actuated ejector vacuum system. Appl Phys Lett 106:031901. https://doi.org/10.1063/1.4906098

Tang S-Y, Ayan B, Nama N, Bian Y, Lata JP, Guo X, Huang TJ (2016) On-chip production of size-controllable liquid metal

microdroplets using acoustic waves. Small 12:3861–3869. https://doi.org/10.1002/smll.201600737

Thelen J, Dickey MD, Ward T (2012) A study of the production and reversible stability of EGaIn liquid metal microspheres using flow focusing Lab. on a Chip 12:3961–3967. https://doi.org/10.1039/C2LC40492C

Utada A, Lorenceau E, Link D, Kaplan P, Stone H, Weitz D (2005) Monodisperse double emulsions generated from a microcapillary device. Science 308:537–541

Wei Z et al (2014) Liquid metal/metal oxide frameworks. Adv Funct Mater 24:3799–3807. https://doi.org/10.1002/adfm.201304064

Wissman J, Dickey MD, Majidi C (2017) Field-controlled electrical switch with liquid metal. Adv Sci (Weinh) 4:1700169. https://doi.org/10.1002/advs.201700169

Yoo K, Park U, Kim J (2011) Development and characterization of a novel configurable MEMS inertial switch using a microscale liquid-metal droplet in a microstructured channel. Sens Actuators A Phys 166:234–240. https://doi.org/10.1016/j.sna.2009.12.008

Yu Y, Wang Q, Yi L, Liu J (2014) Channelless fabrication for large-scale preparation of room temperature liquid metal. Droplets Adv Eng Mater 16:255–262 doi. https://doi.org/10.1002/adem.201300420